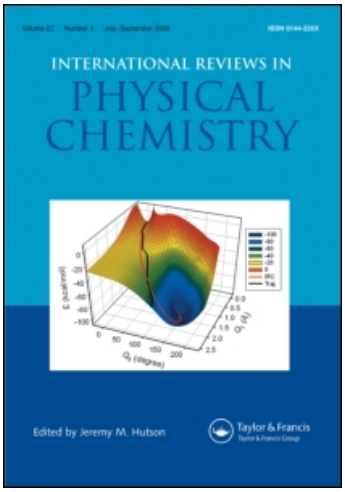

International Reviews in Physical Chemistry
Publication details, including instructions for authors and subscription information:
http://www.informaworld.com/smpp/title~content=t713724383

Charge transfer in collision of N^{2+} and He

Y. Sun[a]; H. R. Sadeghpour[ab]; K. Kirby[a]; A. Dalgarno[a]; G. P. Lafyatis[c]
[a] Harvard-Smithsonian Center for Astrophysics, Cambridge, Massachusetts, USA [b] Department of Physics, The Ohio State University, Columbus, Ohio, USA [c] Institute for Theoretical Atomic and Molecular Physics at Harvard-Smithsonian Center for Astrophysics,

To cite this Article Sun, Y. , Sadeghpour, H. R. , Kirby, K. , Dalgarno, A. and Lafyatis, G. P.(1996) 'Charge transfer in collision of N^{2+} and He', International Reviews in Physical Chemistry, 15: 1, 53 — 64
To link to this Article: DOI: 10.1080/01442359609353174
URL: http://dx.doi.org/10.1080/01442359609353174

INTERNATIONAL REVIEWS IN PHYSICAL CHEMISTRY, 1996, VOL. 15, NO. 1, 53–64

Charge transfer in collision of N^{2+} and He

by Y. SUN, H. R. SADEGHPOUR†, K. KIRBY† and A. DALGARNO
Harvard–Smithsonian Center for Astrophysics, 60 Garden Street, Cambridge, Massachusetts 02138, USA

and G. P. LAFYATIS
Department of Physics, The Ohio State University, Columbus, Ohio 43210, USA

Charge transfer cross-sections in the collision of a doubly-charged nitrogen ion and a helium atom are evaluated with a close-coupling formalism. The charge transfer produces $N^+(^3P)$, $N^+(^1D)$ and He^+ ions via the $^2\Sigma^+$ and $^2\Pi$ molecular states of NHe^{2+}. We describe a method for obtaining a particular diabatic representation from a set of adiabatic dipole moments. Comparison with Landau–Zener model calculations is made and the importance of inner couplings for the production of charge transfer states is demonstrated. Collisional rate coefficients are also obtained. At 10^4 K, the rate coefficient for charge transfer into the ground $N^+(^3P)$ state is about $1{\cdot}3 \times 10^{-10}$ cm^3 s^{-1} and for charge transfer into the metastable $N^+(^1D)$ state $1{\cdot}8 \times 10^{-11}$ cm^3 s^{-1}.

1. Introduction

The charge transfer process

$$N^{2+} + He \rightarrow N^+ + He^+, \tag{1}$$

which produces energetic $N^+(^3P)$ and $N^+(^1D)$ ions, may be of importance as a source of N^+ in astrophysical nebulae and may participate in the chemistry of interstellar molecular clouds subjected to X-rays. The process has been investigated experimentally [1–5] and theoretically [6, 7]. In the theoretical studies, Nikitin and Reznikov [6] and Lafyatis, Kirby and Dalgarno [7] used the Landau–Zener (LZ) model, based respectively on empirical and *ab initio* determinations of the potential energy curves of the cation NHe^{2+}. The two calculations are consistent with each other, given the different estimates of the coupling strength, but disagree significantly with the experimental data on the relative products of $N^+(^1D)$ and $N^+(^3P)$. Since the LZ model may fail at low velocities, we carried out a multi-state close-coupling calculation to investigate the range of its validity and to make comparison with the measurements of the ionic product cross-sections. In §2, the theoretical foundation for this numerical study is laid out and a method for obtaining a particular diabatic representation of Born–Oppenheimer potential energy curves is described. The diabatic potential curves are calculated in a representation which diagonalizes the transition dipole matrix. Cross-sections and collisional rate coefficients calculated using the numerical close-coupling and Landau–Zener approaches are given in §3 and are summarized in §4.

† Also at the Institute for Theoretical Atomic and Molecular Physics at Harvard–Smithsonian Center for Astrophysics.

0144-235X/96 $12·00

2. Theory

The relative motion of the two colliding atoms of energy E, reduced mass μ and nuclear orbital angular momentum N is described by

$$(E-H_{ii})\Psi^N_{ii_0} = \sum_{j\neq i} H_{ij}\,\Psi^N_{ji_0}, \tag{2}$$

where H_{ii} is the Hamiltonian in the electronic state i, $\Psi^N_{ii_0}$ is the ith component of the nuclear wavefunction evolved from the initial state i_0, and H_{ij} are couplings between the ith and jth states. The N^{2+} and He particles interact at large distances in the entrance channel via the long-range polarization potential $-2\alpha_{He}/R^4$, where α_{He} is the static dipole polarizability of a helium atom and R is the internuclear distance, and in the exit channel by the Coulomb repulsion. Asymptotically, $\Psi^N_{ii_0}$ satisfies the outgoing scattering boundary condition

$$\frac{1}{R}\Psi^N_{ii_0}(R) \to k_i^{1/2}[h^-_N(k_i R)\,\delta_{ii_0} - h^+_N(k_i R)\,S^N_{ii_0}], \tag{3}$$

where $h^{\pm}_N$ are spherical Hankel functions in the entrance channel i_0, and Coulomb outgoing/incoming $(+/-)$ functions in the product channels. The kinetic energy of the two atoms in channel i is given by $\hbar^2 k_i^2/2\mu$, and the amplitude for transfer of flux from channel i_0 to channel i is given as the ii_0th element of the S-matrix, S_{ii_0}. The total cross-section at an energy E for transition from state i_0 to i is given by

$$\sigma_{ii_0}(E) = \frac{\pi}{k^2_{i_0}}\sum_N (2N+1)\,|S^N_{ii_0} - \delta_{ii_0}|^2. \tag{4}$$

In order to calculate exactly the scattering wavefunctions in (2), an infinite series of electronic states of NHe^{2+} must be coupled. For low-energy collisions, however, the lowest electronic potential energy states may be grouped separately from the higher energy curves to which they are weakly coupled. The lowest energy adiabatic potential curves, given by Lafyatis *et al.* [7], are shown as solid curves in figures 1(*a*) and 1(*b*). Coupling of these adiabatic channels produces numerical difficulties due to rapid changes in the coupling matrix elements near sharp avoided crossings. To avoid these difficulties, we turn to a diabatic representation for which the potential curves and couplings are smoothly varying functions of the internuclear distance. These two representations are related by a unitary transformation matrix $\mathbf{U}$, given by [8]

$$\mathbf{V}^{\mathrm{d}}(R) = \mathbf{U}^{\mathrm{T}}\mathbf{V}^{\mathrm{a}}(R)\,\mathbf{U}, \tag{5}$$

where $\mathbf{V}^{\mathrm{a,d}}$ are, respectively, the adiabatic and diabatic potential energy matrices. This unitary transformation matrix can be rigorously obtained from

$$\frac{\mathrm{d}\mathbf{U}}{\mathrm{d}R} + \mathbf{P}\mathbf{U} = 0, \tag{6}$$

by defining $\Psi^{\mathrm{d}} = \mathbf{U}^{\mathrm{T}}\Psi^{\mathrm{a}}$. Ψ^{d} and Ψ^{a} are, respectively, finite sets of nuclear wavefunctions in the diabatic and adiabatic representations, and $\mathbf{P}(R)$ is the non-adiabatic radial coupling matrix. Since the coupling between the ion–atom and the ionic pairs vanishes in the asymptotic limit, we require that asymptotically the two representations be equivalent—hence $\mathbf{U}(R\to\infty) = \mathbf{I}$, where $\mathbf{I}$ is the identity matrix.

Since the essential purpose of this transformation is the construction of diabatic states whose properties vary smoothly with R, we claim that an R-dependent unitary

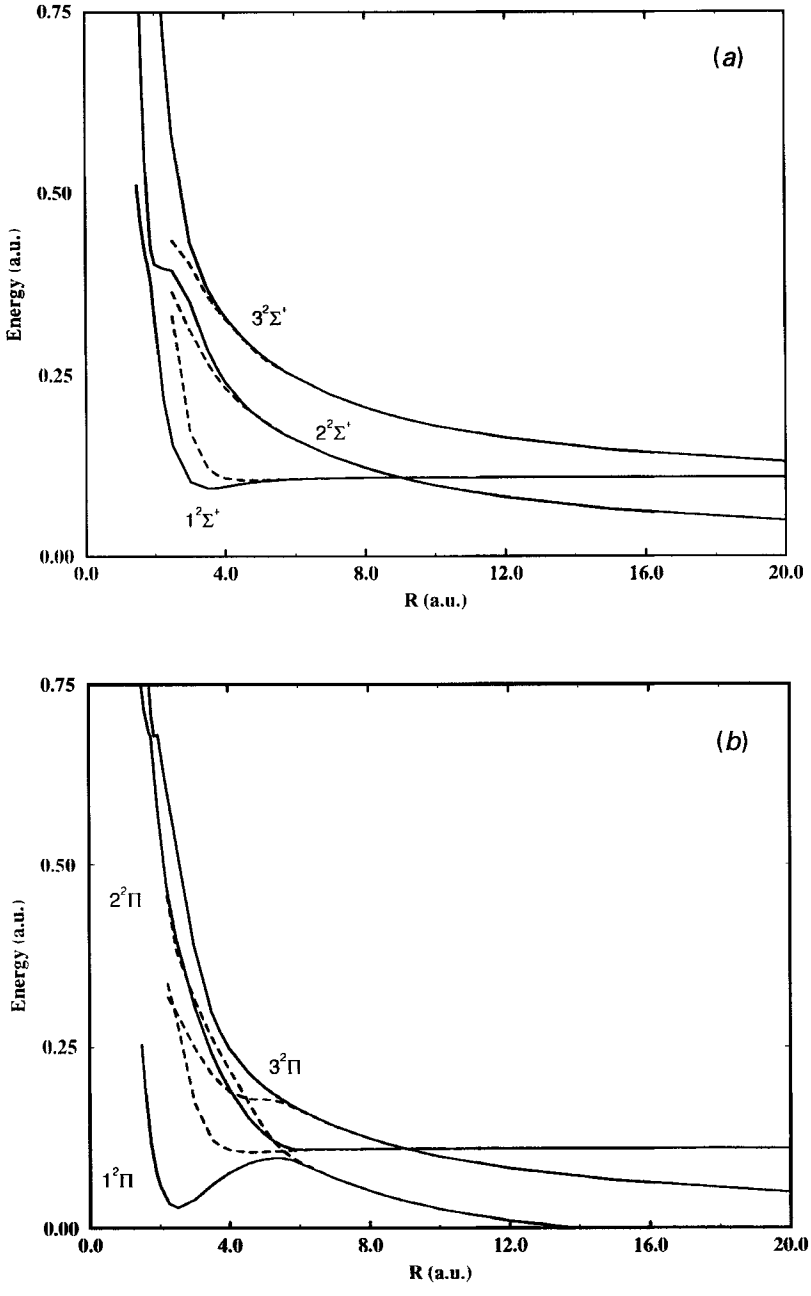

Figure 1. The adiabatic potential energy curves (solid lines) from [7] for the NHe^{2+} molecular symmetries $^2\Sigma^+$ and $^2\Pi$, in (*a*) and (*b*) respectively. The dashed curves are the diabatic potential curves obtained from the transformation in (7). In the separated-atom limit, the $^2\Sigma^+$ curves correlate, in the order of ascending energy, to $N^+(^1D)$, $N^{2+}(^2P^o)$, and $N^+(^1S)$ atomic levels, and the $^2\Pi$ curves correlate to $N^+(^3P)$, $N^+(^1D)$, $N^{2+}(^2P^o)$ levels.

transformation which produces smooth potential energy curves is equivalent in practice to the transformation in (6). Macias and Riera [9] have given a formal theory for calculating diabatic states from R-dependent molecular properties. Werner and Meyer [10] used the representation in which the transition dipole matrix **D** is diagonal to show that for the two-state electron transfer process in the alkali halide, LiF, the two procedures are effectively equivalent. Recently, Li *et al.* [11, 12] used the electric quadrupole operator to obtain diabatic potential curves for the $^3\Pi_g$ and $^3\Sigma_u$ symmetries of molecular oxygen. A rigorous argument has been given by Zygelman (private communication) who has shown that in the limit of infinite-state coupling, the transformations of (6) and (7) are equivalent. It can be shown that a diabatic transformation into a representation in which any operator of the electronic coordinate is diagonal yields the same result. Here, we employ a similar technique and find that the diabatic potential energy curves and coupling elements do indeed vary smoothly with R. We provide a numerical demonstration in support of the near-equivalence of the two diabatic transformations.

3. Results and discussion

The adiabatic dipole moments and the radial coupling matrix elements were calculated using the wavefunctions obtained by Lafyatis *et al.* [7]. They are listed in tables 1–3 as functions of the nuclear separation R for the lowest $^2\Sigma$ and $^2\Pi$ states of NHe^{2+}. The calculations were done with the lighter colliding partner, He, as the centre of reference. The radial coupling matrix elements were evaluated using the Hellman–Feynman theorem.

The unitary matrix $\mathbf{U}_D(R)$ which we used to transform to a diabatic representation was determined by diagonalizing the adiabatic transition dipole matrix $\mathbf{D}(R)$. The new diabatic potential energy matrix is now

$$\mathbf{V}^d(R) = \mathbf{U}_D^T \mathbf{V}^a(R) \mathbf{U}_D. \tag{7}$$

Each column of the unitary transformation matrix $\mathbf{U}_D$ is an eigenvector of the transition dipole matrix, apart from an arbitrary phase factor (± 1). We fixed this phase by requiring that the off-diagonal diabatic potential curves change smoothly with R.

To numerically demonstrate the near-equivalence of the two diabatic representations, we show in figures 2(*a*) and 2(*b*), respectively, the three lowest $^2\Sigma^+$ and $^2\Pi$ diabatic energy curves. The comparison shows that the two representations produce similar potential energy curves. In the case of $^2\Pi$ symmetry illustrated in figure 2(*b*), the two representations differ in the vicinity of the united-atom limit, where the diabatic transformation of (6) yields more attractive curves than the diabatic transformation of (7). The breakdown of both methods is caused by the same deficiency—namely, the restriction of the Hilbert space to a finite size, causing a violation of the closure rule. The discrepancy in figure 2(*b*) in the small-R region occurs because in the three-state approximation we ignore the coupling with higher excited electronic states and restrict the closure to the manifold of only three states. Thus the alternative methods of determining the unitary transformation matrix are equivalent in the sense that whenever it is valid to use a finite set, the methods yield the same results and when they differ, neither is valid. Diabatic potential energies which behave smoothly with R are far more convenient to use than quadrature over the adiabatic couplings.

The diabatic potential energy curves are shown superimposed on the adiabatic

Table 1. Adiabatic dipole moment matrix elements as a function of R in atomic units for the $^2\Sigma^+$ states (the centre of reference is taken at the helium nucleus). The numbers in parentheses represent powers of 10.

R	D^a_{11}	D^a_{22}	D^a_{33}	D^a_{12}	D^a_{13}	D^a_{23}
1·50	−8·51392	−8·06988	−7·70208	−3·43228(−2)	−5·65467(−2)	−5·73333(−1)
1·60	−9·06848	−8·70723	−8·09436	−1·80277(−2)	−5·99921(−2)	−5·03170(−1)
1·75	−9·88460	−9·56991	−8·89306	3·23456(−2)	−1·03843(−1)	−3·64531(−1)
1·80	−1·01441(1)	−9·85332	−9·81456	6·67558(−2)	−1·11314(−1)	−1·48179(−1)
1·90	−1·05404(1)	−1·05274(1)	−1·08618(1)	1·65137(−1)	1·80965(−2)	4·97512(−2)
2·00	−1·09088(1)	−1·12151(1)	−1·14537(1)	9·20192(−2)	1·74818(−1)	−6·22397(−3)
2·25	−1·21195(1)	−1·26232(1)	−1·20219(1)	−4·85493(−2)	9·21614(−1)	−1·32657(−1)
2·50	−1·33279(1)	−1·40773(1)	−1·37169(1)	−2·13381(−1)	1·05057	−1·83032(−1)
3·00	−1·57017(1)	−1·72126(1)	−1·73462(1)	−7·59065(−1)	8·48175(−1)	−1·78956(−1)
3·50	−1·80542(1)	−2·04081(1)	−2·06652(1)	−9·67988(−1)	4·95245(−1)	−1·02338(−1)
3·75	−1·92309(1)	−2·19960(1)	−2·22354(1)	−9·53955(−1)	4·06492(−1)	−8·04265(−2)
4·00	−2·04113(1)	−2·35737(1)	−2·37819(1)	−9·10573(−1)	3·46785(−1)	−6·42627(−2)
4·50	−2·27910(1)	−2·67018(1)	−2·68415(1)	−7·81574(−1)	2·64592(−1)	−3·94998(−2)
4·75	−2·39925(1)	−2·82528(1)	−2·83625(1)	−7·08346(−1)	2·31612(−1)	−2·93990(−2)
5·00	−2·52018(1)	−2·97954(1)	−2·98799(1)	−6·34906(−1)	2·01475(−1)	−2·06685(−2)
5·25	−2·64185(1)	−3·13304(1)	−3·13945(1)	−5·64149(−1)	1·73724(−1)	−1·33441(−2)
5·50	−2·76416(1)	−3·28587(1)	−3·29069(1)	−4·98062(−1)	1·48341(−1)	−7·42025(−3)
5·75	−2·88702(1)	−3·43813(1)	−3·44173(1)	−4·37846(−1)	1·25439(−1)	−2·81625(−3)
7·00	−3·50631(1)	−4·19402(1)	−4·19495(1)	−2·32745(−1)	4·80097(−2)	6·43270(−3)
8·00	−4·00453(1)	−4·79575(1)	−4·79625(1)	−1·74599(−1)	2·01110(−2)	6·60948(−3)
8·50	−4·25416(1)	−5·09608(1)	−5·09670(1)	−2·08209(−1)	1·27662(−2)	6·11707(−3)
8·70	−4·35438(1)	−5·21585(1)	−5·21685(1)	−2·78875(−1)	1·06539(−2)	5·84721(−3)
8·80	−4·40497(1)	−5·27525(1)	−5·27692(1)	−3·71269(−1)	9·76864(−3)	5·65955(−3)
8·90	−4·45795(1)	−5·33227(1)	−5·33700(1)	−6·38016(−1)	9·06889(−3)	5·31093(−3)
8·95	−4·49207(1)	−5·35314(1)	−5·36703(1)	−1·09848	8·92905(−3)	4·82128(−3)
8·98	−4·54105(1)	−5·33716(1)	−5·38505(1)	−2·00834	9·16557(−3)	3·84438(−3)
8·99	−4·59030(1)	−5·29891(1)	−5·39106(1)	−2·71485	9·40822(−3)	2·98763(−3)
9·00	−4·71688(1)	−5·18333(1)	−5·39706(1)	−3·81175	9·72429(−3)	1·24360(−3)
9·02	−5·24586(1)	−4·67634(1)	−5·40908(1)	−3·45701	8·55748(−3)	−4·50523(−3)
9·04	−5·38454(1)	−4·55967(1)	−5·42109(1)	−1·77212	7·20285(−3)	−6·25735(−3)
9·05	−5·40537(1)	−4·54983(1)	−5·42710(1)	−1·37751	6·87776(−3)	−6·52078(−3)
9·08	−5·43787(1)	−4·55033(1)	−5·44512(1)	−7·99852(−1)	6·37627(−3)	−6·75614(−3)
9·10	−5·45282(1)	−4·55738(1)	−5·45713(1)	−6·15812(−1)	6·20259(−3)	−6·75086(−3)
9·20	−5·51632(1)	−4·60387(1)	−5·51719(1)	−2·66627(−1)	5·80473(−3)	−6·33789(−3)
9·50	−5·69723(1)	−4·75296(1)	−5·69737(1)	−7·56407(−2)	5·34108(−3)	−4·82810(−3)
10·00	−5·99754(1)	−5·00261(1)	−5·99763(1)	−2·18931(−2)	4·83146(−3)	−2·97919(−3)
12·00	−7·19831(1)	−6·00180(1)	−7·19836(1)	−7·86966(−4)	3·41594(−3)	−4·06384(−4)
15·00	−8·99892(1)	−7·50115(1)	−8·99895(1)	−1·32149(−5)	2·21856(−3)	−2·08742(−5)
20·00	−1·19994(2)	−1·00007(2)	−1·19994(2)	−7·17696(−7)	1·26223(−3)	−2·39097(−6)
34·00	−2·03998(2)	−1·70002(2)	−2·03998(2)	−4·07490(−8)	4·40484(−4)	−5·24776(−6)

Table 2. Adiabatic dipole moment matrix elements as a function of R in atomic units for the $^2\Pi$ states (the centre of reference is taken at the helium nucleus). The numbers in parentheses represent powers of 10.

R	D^a_{11}	D^a_{22}	D^a_{33}	D^a_{12}	D^a_{13}	D^a_{23}
1·50	−8·87483	−8·12655	−7·61055	−2·20712(−1)	−4·39908(−1)	−4·12654(−2)
1·60	−9·37842	−8·71599	−8·35953	−2·16896(−1)	−4·25241(−1)	−2·72870(−2)
1·75	−1·01129(1)	−9·60096	−9·34809	−2·35161(−1)	−3·57365(−1)	1·00142(−2)
1·80	−1·03533(1)	−9·88759	−9·67229	−2·78148(−1)	−3·01693(−1)	4·62089(−2)
1·90	−1·08294(1)	−1·02885(1)	−1·04903(1)	−3·43810(−1)	1·71465(−1)	2·19949(−2)
2·00	−1·13017(1)	−1·09091(1)	−1·10988(1)	−2·84631(−1)	3·82219(−1)	−3·09666(−2)
2·25	−1·24804(1)	−1·25165(1)	−1·24278(1)	−1·60430(−1)	1·10539	−2·12341(−1)
2·50	−1·36720(1)	−1·42012(1)	−1·36881(1)	−1·73086(−2)	1·26499	−2·42411(−1)
3·00	−1·60961(1)	−1·74962(1)	−1·67868(1)	3·86515(−1)	1·31338	1·54061(−1)
3·50	−1·85496(1)	−2·03801(1)	−2·02167(1)	9·21481(−1)	1·12733	4·08514(−1)
3·75	−1·97835(1)	−2·17660(1)	−2·19144(1)	1·15159	9·82692(−1)	4·16795(−1)
4·00	−2·10254(1)	−2·31763(1)	−2·35590(1)	1·33398	8·45974(−1)	3·84520(−1)
4·50	−2·35690(1)	−2·60263(1)	−2·67282(1)	1·63934	6·31545(−1)	3·07524(−1)
4·75	−2·49130(1)	−2·74044(1)	−2·82789(1)	1·81579	5·45870(−1)	2·81857(−1)
5·00	−2·63784(1)	−2·86698(1)	−2·98174(1)	2·05178	4·66127(−1)	2·69755(−1)
5·25	−2·81224(1)	−2·96621(1)	−3·13473(1)	2·37222	3·83441(−1)	2·76010(−1)
5·50	−3·04610(1)	−3·00636(1)	−3·28708(1)	2·62739	2·82752(−1)	3·02884(−1)
5·75	−3·32677(1)	−2·99998(1)	−3·43896(1)	2·24069	1·65416(−1)	3·23387(−1)
6·00	−3·55367(1)	−3·04757(1)	−3·59045(1)	1·43540	8·17833(−2)	3·07737(−1)
7·00	−4·19321(1)	−3·50702(1)	−4·19402(1)	2·31343(−1)	6·58584(−3)	1·93323(−1)
8·00	−4·79543(1)	−4·00456(1)	−4·79567(1)	5·20869(−2)	9·56073(−4)	1·43821(−1)
8·50	−5·09599(1)	−4·25408(1)	−5·09608(1)	2·59189(−2)	5·16345(−4)	1·66768(−1)
8·70	−5·21618(1)	−4·35410(1)	−5·21604(1)	1·96958(−2)	4·93481(−4)	2·15193(−1)
8·90	−5·33635(1)	−4·45541(1)	−5·33473(1)	1·49864(−2)	7·17075(−4)	4·20938(−1)
9·00	−5·39643(1)	−4·52118(1)	−5·37895(1)	1·29698(−2)	1·85342(−3)	1·25068
9·02	−5·40845(1)	−4·56909(1)	−5·35304(1)	1·23476(−2)	3·18328(−3)	2·16439
9·03	−5·41446(1)	−4·65399(1)	−5·27913(1)	1·15882(−2)	4·89518(−3)	3·21322
9·04	−5·42047(1)	−4·92085(1)	−5·02328(1)	9·26118(−3)	8·25965(−3)	4·45845
9·05	−5·42647(1)	−5·25013(1)	−4·70499(1)	5·42826(−3)	1·09733(−2)	3·57158
9·06	−5·43248(1)	−5·36846(1)	−4·59767(1)	3·23077(−3)	1·16402(−2)	2·31911
9·08	−5·44450(1)	−5·42773(1)	−4·56040(1)	1·61991(−3)	1·16451(−2)	1·23125
9·10	−5·45651(1)	−5·44951(1)	−4·56061(1)	1·03249(−3)	1·13981(−2)	8·12718(−1)
9·20	−5·51659(1)	−5·51612(1)	−4·60399(1)	2·99710(−4)	9·99571(−3)	2·74472(−1)
9·50	−5·69680(1)	−5·69709(1)	−4·75301(1)	4·85566(−5)	6·68511(−3)	6·92109(−2)
10·00	−5·99711(1)	−5·99741(1)	−5·00266(1)	6·50933(−6)	3·43122(−3)	1·93556(−2)
12·00	−7·19800(1)	−7·19821(1)	−6·00183(1)	−3·72340(−8)	2·44023(−4)	6·82870(−4)
15·00	−8·99872(1)	−8·99886(1)	−7·50117(1)	−3·31610(−8)	4·93979(−6)	1·03649(−5)
20·00	−1·19993(2)	−1·19994(2)	−1·00007(2)	−2·02752(−8)	7·05905(−8)	2·05441(−7)

Table 3. Adiabatic radial coupling T-matrix elements as a function of R in atomic units for the $^2\Sigma^+$ and $^2\Pi$ states, where T is related to P by Hellman–Feynman theorem as [9] $P_{ij} = 2(E_j - E_i)^{-1}T_{ij}$. The adiabatic potential energies E_1, E_2 and E_3 are given by Lafyatis *et al.* [7]. The centre of reference is taken at the helicum nucleus. The numbers in parentheses represent powers of 10.

	$^2\Sigma^+$			$^2\Pi$		
R	T_{12}	T_{23}	T_{23}	T_{12}	T_{13}	T_{23}
1·50	1·33165(−2)	−1·65235(−1)	6·57162(−3)	2·95937(−2)	1·10649(−3)	1·15950(−1)
1·60	1·00413(−2)	−1·40894(−1)	1·36285(−2)	4·15210(−2)	−3·21706(−3)	7·31929(−2)
1·75	−2·51282(−4)	−1·04595(−1)	4·04111(−2)	7·73324(−2)	−3·23688(−2)	3·32867(−2)
1·80	−1·37029(−2)	−9·25682(−2)	8·54423(−2)	1·03242(−1)	−7·69718(−2)	2·92692(−2)
1·90	−7·26436(−2)	−1·23317(−2)	4·99370(−2)	1·66755(−1)	−6·08758(−2)	6·24554(−2)
2·00	−5·78673(−2)	3·16645(−2)	2·53277(−2)	8·48510(−2)	−7·40188(−3)	7·23692(−2)
2·25	−2·91733(−2)	1·46662(−1)	3·85612(−2)	1·67091(−2)	9·58201(−2)	−2·49745(−2)
2·50	−1·12355(−2)	1·19718(−1)	3·76990(−2)	−3·35271(−3)	8·38078(−2)	−4·64229(−2)
3·00	6·11012(−3)	6·14849(−2)	2·75429(−2)	2·63799(−2)	4·33829(−2)	−3·99355(−2)
3·50	9·26037(−3)	2·74405(−2)	1·94711(−2)	−2·28685(−2)	2·01146(−2)	−1·22090(−2)
3·75	7·33350(−3)	1·83756(−2)	1·47846(−2)	−1·84414(−2)	1·51945(−2)	−6·03669(−3)
4·00	4·58836(−3)	1·26668(−2)	1·07993(−2)	−1·45751(−2)	1·20020(−2)	−2·61704(−3)
4·50	−6·67777(−4)	6·65730(−3)	5·73675(−3)	−8·91474(−3)	7·90734(−3)	3·76879(−4)
4·75	−2·99146(−3)	4·95659(−3)	4·29016(−3)	−6·92440(−3)	6·45269(−3)	9·41664(−4)
5·00	−5·35970(−3)	3·66300(−3)	3·32113(−3)	−5·35457(−3)	5·24525(−3)	1·20224(−3)
5·25	−8·04097(−3)	2·58833(−3)	2·71735(−3)	−4·11855(−3)	4·23611(−3)	1·28220(−3)
5·50	−1·06085(−2)	1·58791(−3)	2·36971(−3)	−3·14735(−3)	3·39388(−3)	1·25919(−3)
5·75	−1·02914(−2)	7·11124(−4)	2·04239(−3)	−2·38676(−3)	2·69573(−3)	1·18185(−3)
6·00	−7·29169(−3)	2·30761(−4)	1·61303(−3)	−5·04861(−4)	7·59638(−4)	6·76912(−4)
7·00	−1·50445(−3)	−1·55772(−5)	4·71104(−4)	−7·03258(−5)	2·50913(−4)	4·15073(−4)
8·00	−3·80990(−4)	−5·34770(−6)	7·65100(−5)	5·70301(−5)	1·43115(−4)	3·28641(−4)
8·50	−1·95877(−4)	−3·40275(−6)	−3·28385(−5)	1·43132(−4)	1·16168(−4)	2·99650(−4)
8·70	−1·50308(−4)	−3·42382(−6)	−9·77743(−5)	2·32712(−4)	1·06678(−4)	2·85725(−4)
8·90	−1·15330(−4)	−5·26873(−6)	−2·92228(−4)	4·69915(−4)	1·03592(−4)	2·70679(−4)
9·00	−1·00178(−4)	−1·40976(−5)	−1·01053(−3)	8·67756(−4)	1·12023(−4)	2·59519(−4)
9·02	−9·54489(−5)	−2·43999(−5)	−1·79704(−3)	1·65004(−3)	1·35971(−4)	2·43046(−4)
9·03	−8·97043(−5)	−3·76562(−5)	−2·70182(−3)	2·25892(−3)	1·56779(−4)	2·28517(−4)
9·04	−7·17992(−5)	−6·37467(−5)	−3·79808(−3)	3·21136(−3)	1·94581(−4)	1·95417(−4)
9·05	−4·22032(−5)	−8·48358(−5)	−3·08186(−3)	2·98426(−3)	2·69027(−4)	4·68738(−5)
9·06	−2·52172(−5)	−9·00357(−5)	−2·02769(−3)	1·56631(−3)	2·69921(−4)	−1·66190(−5)
9·08	−1·27571(−5)	−9·01579(−5)	−1·10335(−3)	1·23165(−3)	2·67592(−4)	−2·86505(−5)
9·10	−8·20782(−6)	−8·83027(−5)	−7·45885(−4)	7·39594(−4)	2·61537(−4)	−4·42059(−5)
9·20	−2·51486(−6)	−7·76891(−5)	−2·80994(−4)	5·81852(−4)	2·58256(−4)	−4·81793(−5)
9·50	−5·35754(−7)	−5·23538(−5)	−9·13627(−5)	2·78286(−4)	2·45305(−4)	−5·10059(−5)
10·00	−1·44037(−7)	−2·71382(−5)	−3·38273(−5)	9·98853(−5)	2·15249(−4)	−3·84303(−5)
12·00	−6·81868(−8)	−2·01443(−6)	−1·93571(−6)	3·77180(−5)	1·75849(−4)	−2·09865(−5)
15·00	−4·66683(−8)	−5·68788(−8)	−3·95151(−8)	2·18037(−6)	8·60686(−5)	−1·35381(−6)
20·00	−2·96604(−8)	−6·44924(−10)	−1·62929(−9)	4·90004(−8)	3·59773(−5)	1·20837(−8)

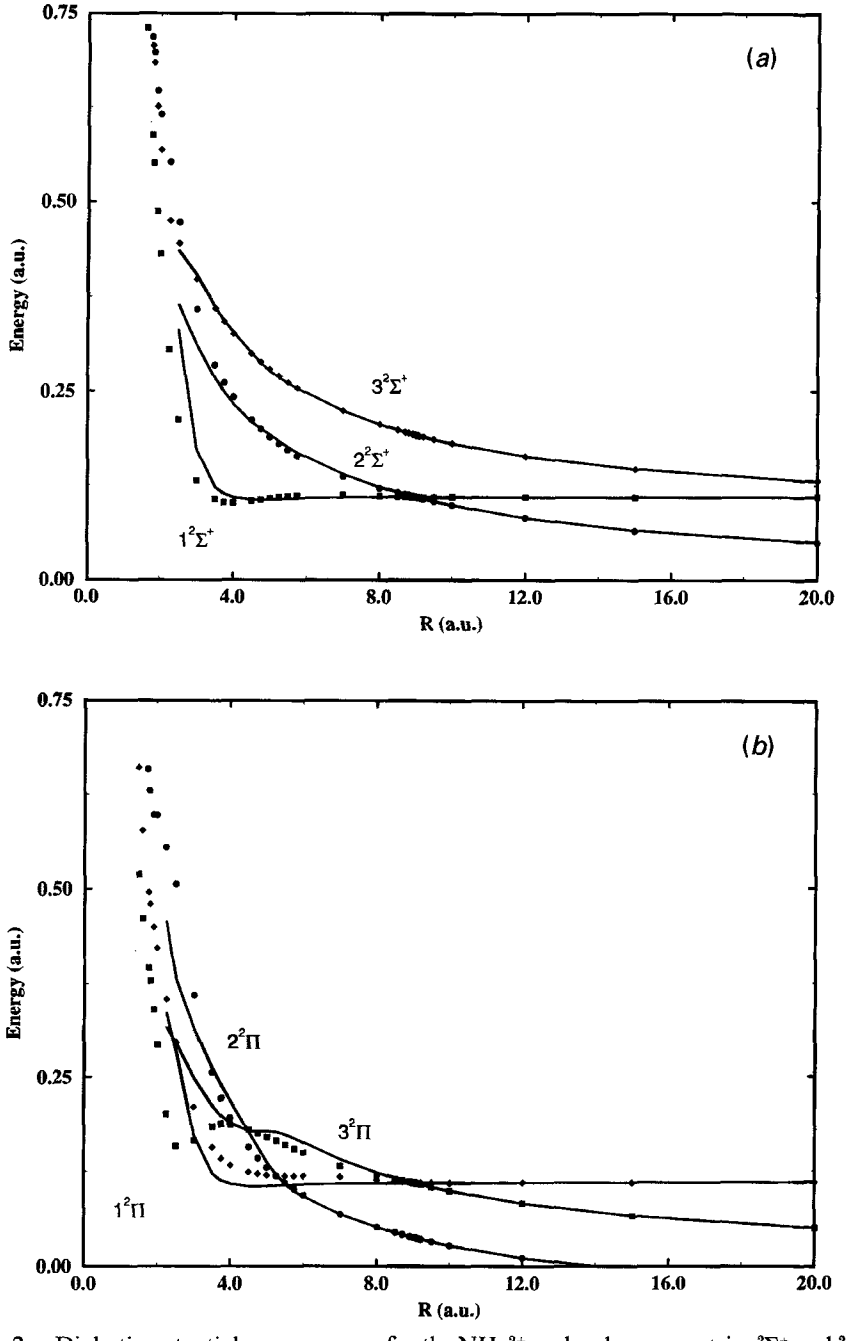

Figure 2. Diabatic potential energy curves for the NHe^{2+} molecular symmetries $^2\Sigma^+$ and $^2\Pi$, in (*a*) and (*b*) respectively. The curves in symbols are the potential curves obtained from the transformation in (6), and the solid curves are the same diabatic curves as in figure 1, shown here for visual comparison.

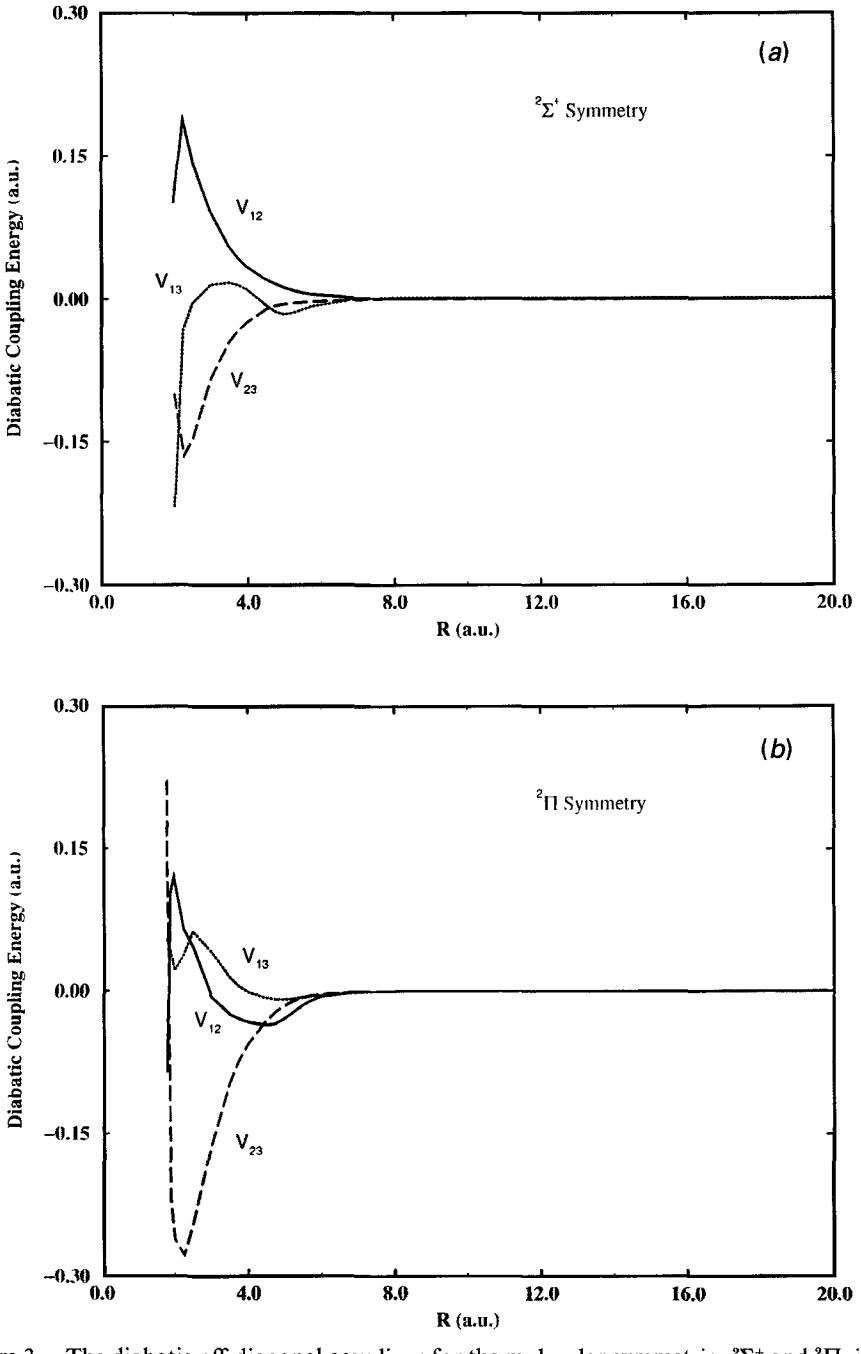

Figure 3. The diabatic off-diagonal couplings for the molecular symmetries $^2\Sigma^+$ and $^2\Pi$, in (*a*) and (*b*) respectively. The indices are the same as those used in figures 1 and 2.

curves of [7], in figures 1(*a*) and 1(*b*), as dashed curves, and the off-diagonal diabatic curves obtained by applying the transformation $\mathbf{U}_D(R)$ are shown in figures 3(*a*) and 3(*b*). The strong couplings in the intermediate region lead to quite different shapes for the potential energy curves of the adiabatic and diabatic $^2\Pi$ states.

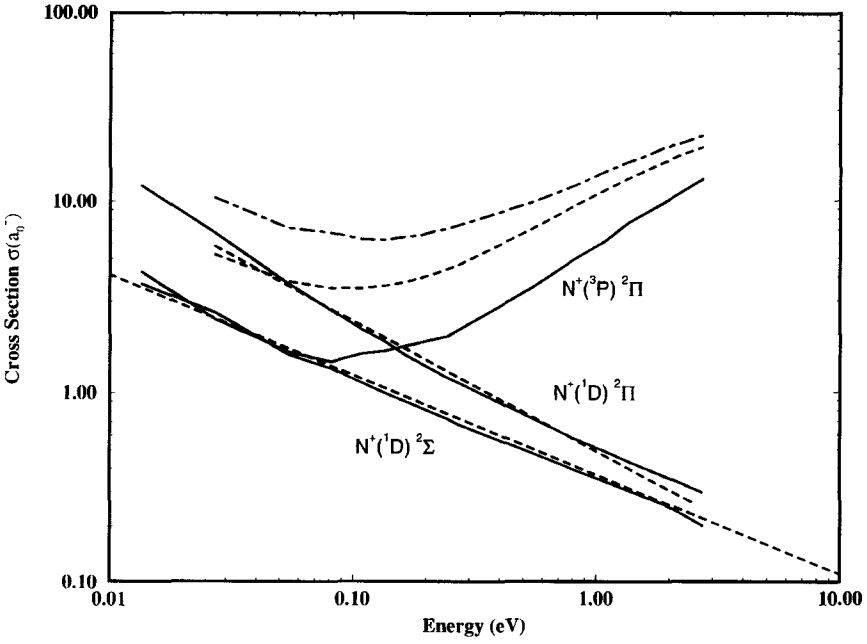

Figure 4. The partial cross-sections for the charge transfer processes leading to the production of $N^+(^3P)$ and $N^+(^1D)$ final states. The solid curves are the present close-coupling results, and the dashed curves are the linear Landau–Zener cross-sections from (8). The dotted–dashed curve is the close-coupling calculation with the intermediate coupling near $R = 4{\cdot}8a_0^3$ in the $^2\Pi$ symmetry turned artificially off.

We employed the renormalized Numerov method [13] to obtain the solutions of (2) subject to the boundary conditions in (3), and to determine the scattering matrix $S^N_{ii_0}$. We also calculated the charge transfer cross-sections in the multi-state Landau–Zener approximation. In the LZ model, the charge transfer cross-section at an energy E is written in terms of P_{ii_0}, the probability of entering in a channel i_0 and exiting in channel i, as

$$\sigma_{ii_0}(E) = \frac{\pi g_{i_0}}{k_i^2} \sum_N (2N+1) P_{ii_0}, \tag{8}$$

where g_{i_0} is the probability of particle approach along the electronic state i_0. For approach along the entrance ($N^{2+} + He$) $^2\Pi$ and $^2\Sigma^+$ channels, $g_{i_0} = \frac{2}{3}$ and $g_{i_0} = \frac{1}{3}$ [7]. Labelling successively the lowest three asymptotic adiabatic channels by subscripts 1, 2 and 3, the total probability leading to singly-charged product ions $N^+(^1D)$ and $N^+(^3P)$ in the $^2\Pi$ symmetry is then given as

$$P_{23} = p_{23}(1-p_{23})[1+p_{12}^2+(1-p_{12})^2], \tag{9a}$$

and

$$P_{13} = 2p_{23}p_{12}(1-p_{12}), \tag{9b}$$

where p_{23} is the local LZ diabatic transition probability near the crossing at $9a_0$ and p_{12} is the probability for crossing at $5{\cdot}5a_0$. For the $^2\Sigma^+$ molecular symmetry, the LZ charge transfer probability is described in the two-state approximation as

$$P_{12} = 2p_{12}(1-p_{12}), \tag{10}$$

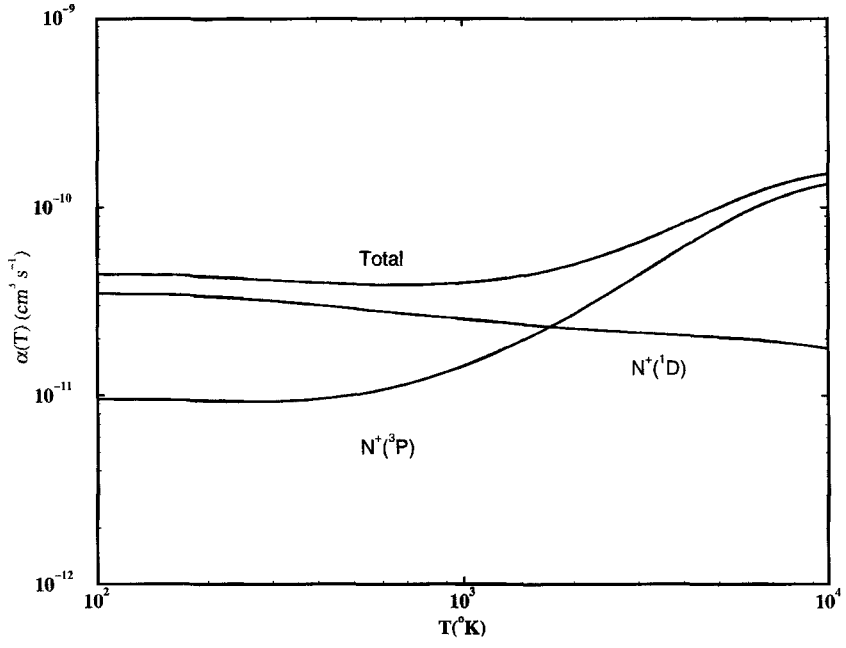

Figure 5. Collisional rate coefficients for producing ground and metastable nitrogen ions, $N^+(^3P)$ and $N^+(^1D)$.

where p_{12} is the local LZ diabatic transition probability near the crossing at $9a_0$ between the channels 1 and 2. We note that in (9*a*) the total probability for producing the metastable nitrogen ion is independent of the transition probability at $R = 5{\cdot}5a_0$ in the extremes of fully adiabatic ($p_{12} = 0$) or totally diabatic ($p_{12} = 1$) passage.

The results of the three-state LZ and coupled-channel calculations are shown in figure 4 for the two molecular symmetries. Close agreement between the two calculations exists for the production of $N^+(^1D)$ states, while the discrepancy between the results for the case of $N^+(^3P)$ state production is at times up to 30%, although the two calculations converge as collision energies increase. This discrepancy arises from the nature of the avoided crossings. For the $^2\Pi$ and $^2\Sigma^+$ channels leading to the $N^+(^1D)$ charge state, the crossing near $9a_0$ dominates low-energy collisions. The charge transfer process in this case is driven by the isolated crossing at $9a_0$. The influence of the intermediate crossings is masked because the nuclear wavefunctions for the production of $N^+(^1D)$ are ineffective in tunnelling through the inner centrifugal barrier. Thus, the close-coupling calculations yield similar results to the semi-classical Landau–Zener calculation. In contrast, for the $^2\Pi$ channel leading to $N^+(^3P)$, the intermediate couplings at $5{\cdot}5a_0$ and nearby $4{\cdot}8a_0$ play a dominant role in the charge transfer process. Although the present LZ model includes the coupling of three states, the crossing at $4{\cdot}8a_0$ in figure 1 (*b*) plays no role because it is classically inaccessible at low energies. Accordingly, we expect the LZ results to be different from the coupled-channel calculation. To corroborate this conjecture, we performed another coupled-channel calculation with the coupling strength near $4{\cdot}8a_0$ set to zero. This increased the charge transfer flux in the $N^+(^3P)$ channel, as shown in figure 4. There is a discrepancy between the present $N^+(^3P)$ LZ cross-sections and those given by Lafyatis *et al.* [7]. It occurs because the latter calculations were carried out using the coupling information near the $5{\cdot}5a_0$, obtained from the *adiabatic* curves of figure 1. The presence of a strong coupling near $4{\cdot}8a_0$ drastically changes the form and shape of the potential curves in

its vicinity, as manifested by the noticeable differences in the adiabatic and diabatic curves.

The corresponding rate coefficients for producing $N^+(^3P)$ and $N^+(^1D)$ are shown in figure 5. The Landau–Zener and close-coupling calculations are qualitatively consistent with the measurements at an impact energy of 1 keV of Hormis *et al.* [2] and with the measurements at lower energies of Sadilek *et al.* [5] in showing an enhanced relative production of ground state ions at high energies. However, there is a substantial quantitative disagreement between the cross-section ratio for capture into the ground and metastable states measured at energies of a few eV [5] and the theoretical results. A recent measurement of the total charge transfer rate coefficient by Fang and Kwong (private communication) at about 6000 K agrees well with our calculated value of $1{\cdot}1 \times 10^{-10}$ cm^3 s^{-1}.

4. Summary

This work reports the evaluation of the low-energy single charge transfer cross-sections in a typical collision of an ion–atom pair, NHe^{2+}. For the calculations, we used a particular transformation which provided a smooth diabatic Born–Oppenheimer potential energy matrix, thereby avoiding the numerical instabilities resulting from integration over a rapidly-changing radial coupling matrix. The *R*-dependent property we used was the set of electric dipole moments. The diagonal and off-diagonal potential energy curves obtained from this transformation behave smoothly with *R*. The low-energy partial and total cross-sections were evaluated by coupling these diabatic channels and are compared with linear Landau–Zener transition cross-sections. We also explored the range of validity of the LZ approximation and demonstrated the importance of avoided crossings at intermediate internuclear separations. The discrepancy with experimental data [5] persists.

Acknowledgments

Support for this work was provided by a grant from the US Department of Energy, Division of Chemical Sciences, Office of Basic Energy Sciences, Office of Energy Research. Support for the Institute for Theoretical Atomic and Molecular Physics was provided by a grant from the National Science Foundation.

References

[1] Sato, Y., and Moore, J. H., 1979, *Phys. Rev.* A, **19**, 95.
[2] Hormis, W. G., Kamber, E. Y., and Hasted, J. B., 1986, *Int. J. Mass Spectrom. Ion Processes*, **69**, 211.
[3] Sharma, S., Awad, G. L., Hasted, J. B., and Mather, D., 1979, *J. Phys.* B, **12**, L163.
[4] Lennon, M., McCulloch, R. W., and Gilbody, H. B., 1983, *J. Phys.* B, **16**, 2119.
[5] Sadilek, M., Vancura, J., Farnik, M., and Herman, Z., 1990, *Int. J. Mass Spectrom. Ion Processes*, **100**, 197.
[6] Nikitin, E. E., and Reznikov, A. I., 1992, *Molec. Phys.*, **77**, 563.
[7] Lafyatis, G. P., Kirby, K., and Dalgarno, A., 1993, *Phys. Rev.* A, **48**, 321.
[8] Heil, T. G., Butler, S. E., and Dalgarno, A., 1981, *Phys. Rev.* A, **23**, 1100.
[9] Macias, A., and Riera, A., 1978, *J. Phys.* B, **11**, L489.
[10] Werner, H.-J., and Meyer, W., 1981, *J. chem. Phys.*, **74**, 5802.
[11] Li, Y., Honigmann, M., Hirsch, G., and Buenker, R. J., 1993, *Chem. Phys. Lett.*, **212**, 185.
[12] Li, Y., Honigmann, M., Bhanuprakash, K., Hirsch, G., and Buenker, R. J., 1992, *J. chem. Phys.*, **96**, 8314.
[13] Johnson, B. R., 1978, *J. chem. Phys.*, **69**, 4678.